Materials Today Sustainability 19 (2022) 100171

Contents lists available at ScienceDirect

Materials Today Sustainability

journal homepage: https://www.journals.elsevier.com/materials-today-sustainability

Sustainable generator and *in-situ* monitor for reactive oxygen species using photodynamic effect of single-walled carbon nanotubes in ionic liquids

X. Huang [a], E. Witherspoon [b], Y. Li [c], S. Ward [b], J. Yu [d], H.F. Wu [e], H. Ding [f], Q. Li [c, *], Z. Wang [b, *], P. Dong [a, *]

[a] Department of Mechanical Engineering, George Mason University, Fairfax, VA 22030, USA
[b] Department of Chemistry, Oakland University, Rochester Hills, MI 48309, USA
[c] Department of Electrical and Computer Engineering, George Mason University, Fairfax, VA 22030, USA
[d] Nanotechnology Systems Division, Hitachi High-Tech America, Inc. 22610 Gateway Center Drive, Clarksburg, MD 20871, USA
[e] U.S. Department of Energy, Washington, DC 20585, USA
[f] Idaho National Laboratory, Idaho Falls, ID 83415, USA

ARTICLE INFO

Article history:
Received 7 March 2022
Received in revised form
14 May 2022
Accepted 25 May 2022
Available online 31 May 2022

Keywords:
Electrochemistry
Superoxide
Detection
Irradiation
Sustainability

ABSTRACT

Due to the increasing concerns regarding public health and climate change, disinfectant generator technologies that utilize green processes are becoming necessary. It has been confirmed that single-walled carbon nanotubes (SWCNTs) can generate reactive oxygen species (ROS) in aqueous media when illuminated with solar irradiation. However, low efficiency due to competitive reactions between ROS and water and unclear kinetics hinder their potential practical applications. To overcome these limitations, here, SWCNTs were studied in a non-aqueous ionic liquid (IL) to form a suspension system for generating superoxide (O_2^-) under UV light. The as-obtained O_2^- from SWCNTs was qualitatively confirmed by electron paramagnetic resonance and UV–vis spectroscopy. The sustainability of the new SWCNTs/IL system was confirmed by UV–vis and Fourier-transform infrared spectroscopy. The IL proved to be an ideal media that could extend the lifetime of O_2^- from a few microseconds (generated in water) to at least 65 h in the IL. The kinetics of photodynamic effect were investigated by electrochemical characterizations. A new method was established to *in-situ* monitor the O_2^- level in the IL system. The O_2^- level in the IL was quantitatively determined by combining cyclic voltammetry and chronoamperometry techniques. The SWCNTs/IL system generated 4.11 mM of O_2^- in a mini-scale generator, which was in excess of germicidal levels for ROS. The sustainable, long duration and high-yield of the generator exhibited excellent potential as a generator as well as an *in-situ* monitor for O_2^-. This work could pave the way for O_2^- generation using SWCNTs and promote its applications in air and water disinfection for public health, as well as O_2^- sensitive chemical sensors for monitoring the environmental quality.

1. Introduction

Recently, public health has become one of the top research interests. Traditionally, methanol, ethyl alcohol, and isopropyl alcohol have been used to prevent disease from spreading since they are fast-acting and effective; however, they are limited by short-term use due to high volatility. As such, it is necessary to develop sustainable disinfectants which utilize green processes and feedstock and are sufficient for long-term use. Reactive oxygen species (ROS) are a type of highly reactive molecules that include, singlet oxygen ($^1O_2$), hydroxyl radical (HO•), superoxide (O_2^-), and hydrogen peroxide (H_2O_2). Plenty of ROS-based disinfection technologies have been developed to kill viruses, bacteria, or deactivate proteins [1–3]; however, in practice, generating ROS in aqueous media comes with low yield, high cost, fast decay, and difficult storage [3–5]. Thus, these limitations must be addressed for widespread application to become viable.

Single-walled carbon nanotubes (SWCNTs) have attracted increasing attention due to their excellent mechanical, electrical,

* Corresponding authors.
E-mail addresses: qli6@gmu.edu (Q. Li), zhewang@oakland.edu (Z. Wang), pdong3@gmu.edu (P. Dong).

https://doi.org/10.1016/j.mtsust.2022.100171
2589-2347/

thermal, and optical properties, which enable several applications in multiple fields, such as coatings and films, microelectronics, energy storage, biosensing, and water treatment [6–15]. It has been proven that SWCNTs can generate ROS in the presence of UV or visible light in water [16–20]. When the presence of SWCNTs are excited by photo illumination in liquid media, a free electron is released by the photoexcited SWCNTs and captured by oxygen (O_2), and O_2^- is produced (Fig. 1) [16]. O_2^- can further be reduced to HO• and H_2O_2 in the presence of protons [21]. This process is known as the photodynamic effect of SWCNTs.

The efficiency of the photodynamic effect of SWCNTs is dependent upon the SWCNTs having either semiconducting or metallic properties, which is determined by the arrangement of carbon atoms (chirality). When SWCNTs are irradiated, the electrons in the valence band transition to the conduction band and can react with other active substances. As shown in Fig. 1, the semiconducting carbon nanotubes have a smaller optical transition gap and more optical transition path than metallic CNTs. To overcome the band gaps of E_{11} (Fig. 1), the irradiation wavelength should be in the range of 900 nm–1400 nm and 550 nm–900 nm, respectively [22]. The specific ideal wavelength depends on the chirality of each SWCNT. Conversely, overcoming the bandgap of M_{11} (Fig. 1) requires lower wavelength irradiation (350 nm–650 nm) [22]. Although the presence of metallic SWCNTs may relax the electrons away from semiconducting SWCNTs, it has been reported that a mixture type of semiconducting and metallic SWCNTs could also generate ROS when using a 350 nm UV light [17]. This suggested the efficiency of the electron utilized by O_2 was higher than that relaxed by metallic SWCNTs in the competition, especially when semiconducting SWCNTs are dominant in the composition. In addition, 975.5 nm near infrared light has also been used to excite SWCNTs and successfully generate ROS [16]. Most SWCNTs on the market are offered in a mixture of metallic and semiconducting carbon nanotubes; it remains a challenge to obtain high purity SWCNTs with specific chirality. To ensure all SWCNTs, regardless of chirality, would be excited, a 350 nm UV light source was used herein. After being excited, SWCNTs can convert photon energy to fluorescence emission heat energy or trigger photodynamic reactions, which activate the adsorbed oxygen to produce ROS. The occurrence of photodynamic reactions is determined by the structure of SWCNTs [23].

Currently, ROS can be detected by several techniques such as chromatography, spectrophotometry, and electrochemistry, with the help of different chemical scavengers or indicators [24]. For example, $^1O_2$ can be detected by furfuryl alcohol through high-performance liquid chromatography [17]. O_2^- is commonly detected using nitro blue tetrazolium salt (NBT^{2+}), which reacts with O_2^- to produce monoformazan, a purple substance with optical absorption at 530 nm in water. This method is convenient and fast, but NBT^{2+} is vulnerable to other reactive substances and is unsuitable for low-level detection [24]. Terephthalic acid (TPA) is a convenient detector for HO•. The non-fluorescent TPA becomes fluorescent monohydroxy terephthalate upon reaction with HO•. The production can be excited at around 315 nm and emission is seen at 425 nm by using a fluorescence meter [25]. This method is low-cost and fast, but TPA is also sensitive to UV light, which turns the sample fluorescent in a UV-dependent system. Electrochemical methods can be used to selectively detect O_2^-. O_2^- reacts with certain proteins, and these reacted proteins can be re-oxidized at a specific potential. However, only a limited number of sensitive proteins are available for O_2^- and additional preparation for the proteins is required [24]. Here, we propose an *in-situ* and accurate detection method for ROS, specifically O_2^-, based on the principal of electrochemistry without needing additional indicators, equipment, or complicated sample preparation.

Although CNT-generated ROS have been investigated in many conditions, most reported results were studied in aquatic environments [16–18], when ROS usually have very short lifetimes. For instance, $^1O_2$ only lasts for 4 μs in water [4]. The lifetime of O_2^- is also very short, only about 1 min if existing in basic aqueous solution [5]. ROS can quickly react with hydrogen ions (protons) in the environment to form stable substances. For example, O_2^- reacts with hydrogen to produce H_2O_2 [16]. Meanwhile, the HO• radical can be consumed by organic compounds, carbonates, or other ROS quenchers within a few microseconds [26]. The combination of these factors has thus far limited the kinetic studies of the

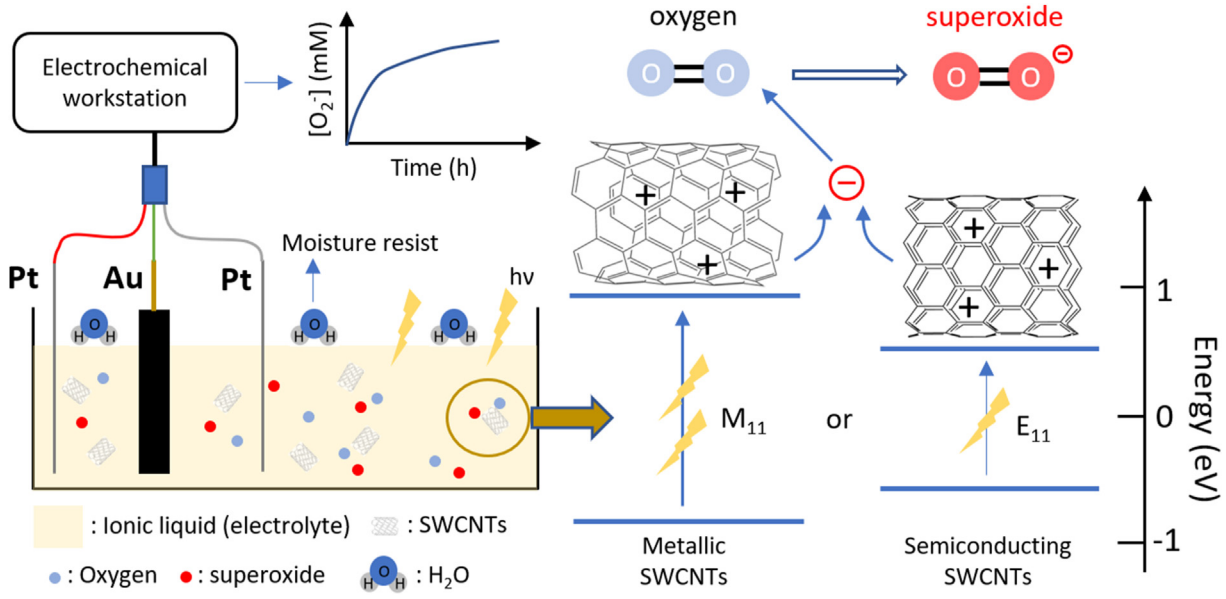

Fig. 1. Schematic for O_2^- generation by SWCNTs under photo illumination in IL and the *in-situ* O_2^- detection by electrochemical measurements. IL, ionic liquid; SWCNT, single-walled carbon nanotube.

generation process and its applications. This remains a major challenge in further designs of energy-efficient systems which yield high concentrations of ROS and are able to sustain long-term use. Accordingly, it is critical to find an inert solvent to study the generation process that will not participate in reactions, or, ideally, will lower the rate of the reactions, in order to resolve these problems. Thus, rather than water, which is protic, we chose to study these phenomena using an aprotic solvent.

Considering the inert and low volatility nature, aprotic ionic liquid (IL) is an excellent solvent to study the properties of O_2^- [27–29]. As one of the most common room-temperature ILs, 1-butyl-1-methylpyrrolidinium bis(trifluoromethylsulfonyl)imide ([C_4mpy] [NTf_2]) has two roles in our system (Fig. 1). First, its hydrophobicity helps to isolate moisture from ROS products, which creates an inert environment for ROS to exist in. It has been reported that O_2^- could exist in [C_4mpy] [NTf_2] for over 9 h [30]. Second, this IL is especially useful due to its excellent electrochemical properties when used as an electrolyte [31,32]. The redox couple, O_2/O_2^-, can be generated during cyclic voltammetry (CV). Wang et al. [28] reported the oxidation peak for O_2^- was found near −1.2 V vs. ferricenium/ferrocene (Fc^+/Fc) couple during the reverse CV scan at a Pt electrode. It is known the height of oxidation peak is related to the concentration of reactant, O_2^- [33]. This means that electrochemical methods can be used to study ROS generation in IL without introducing any additional indicators or quenchers.

In this work, the photodynamic effect of SWCNTs was investigated in [C_4mpy] [NTf_2]. The SWCNTs/IL system was illuminated with UV light to produce O_2^-. The sustainability of the system was studied using UV–vis and Fourier-transform infrared (FT-IR) spectroscopy. Moreover, the generation of O_2^- was qualitatively confirmed using electron paramagnetic resonance (EPR) and UV–vis spectroscopy. To *in-situ* monitor the O_2^- concentration changes in the IL, a new detection method was established using CV. Finally, the concentration of O_2^- was quantitatively determined by conventional electrochemical methods. It is expected that this work will provide new insights into water and air disinfection fields.

2. Materials and methods

2.1. Materials

SWCNTs (>95%) were purchased from Sigma-Aldrich. 1-Butyl-1-methylpyrrolidinium bis(trifluoromethylsulfonyl)imide ([C_4mpy] [NTf_2], 99.5%) was purchased from IOLITEC GmbH company. NBT chloride was purchased from Fisher scientific. Sodium dodecyl sulfate (SDS) was purchased from Sigma-Aldrich (ACS reagent, ≥99.0%). Deionized water (18.2 MΩ cm resistivity at 25 °C) was produced by Milli-Q Reference Water Purification System.

2.2. Optical spectra characterizations for SWCNTs by UV–vis spectroscopy

A UV–Vis spectrophotometer (GENESYS 150) was used to characterize the optical absorption of SWCNTs from 300 nm to 1100 nm. To prepare the suspension for UV–Vis spectroscopy, 3 mg of the as-received SWCNTs were added to 100 mL of 2 wt% SDS aqueous solution. The solution was then dispersed by probe sonication (Q500, Qsonica, LLC) in an ice bath for 30 min using a power of 100 Watts. After that, the dispersed SWCNTs in SDS aqueous solution were stabilized at room temperature and used as the analyte sample. A 100 mL of 2 wt% SDS aqueous solution without SWCNTs was also prepared and used as the benchmark.

2.3. Qualitative determination of O_2^- by EPR

EPR spectroscopy was used to characterize the existence of O_2^- in the IL. Prior to EPR spectroscopy measurements, 0.1 mL of SWCNTs were added to 1.5 mL of [C_4mpy] [NTf_2] and stirred. Oxygen was then bubbled throughout the suspension and illuminated with UV light for 22 h. EPR studies were carried out using a Bruker EMXplus-9.5/2.7/P/L X-band continuous wave spectrometer (100 kHz field modulation, 3.2 G modulation amplitude at 45 dB) at 77 K. After the generation of O_2^-, the solution was quickly transferred to an EPR sample tube and frozen in liquid N_2. No further adjustments were made before scanning.

2.4. Qualitative determination of O_2^- by UV–vis spectroscopy using NBT^{2+}

To prepare the suspension for characterizing the O_2^- scavenger, 1 mg of as-received SWCNTs were added to 100 mL of ethanol to form a 10 mg/L suspension of ethanol and SWCNTs. The solution was then dispersed by probe sonication in an ice bath for 30 min using a power of 100 Watts. Finally, the suspension of ethanol and SWCNTs was obtained and stored in the dark until further use. NBT^{2+} salt was used to detect the O_2^-. 1 mg NBT^{2+} was added to 1 mL IL and stirred for 30 min. The composition of analytes contained 0.1 mL NBT^{2+}/IL suspension, 0.4 mL IL and 0.05 mL ethanol/SWCNTs suspension. Semimicro UV cuvettes were used to hold the samples. The reference sample did not contain any NBT^{2+}. The samples for control groups did not contain any SWCNTs. The samples were illuminated with 350 nm UV light (6 Watts) and characterized using UV–Vis spectroscopy every 2 h. The details for the composition of each sample will be given in the discussion section.

2.5. Molecular structure characterization for IL using FT-IR spectroscopy

FT-IR absorption spectra of SWCNTs/IL suspension were recorded using a Varian 3100 Excalibur Series Spectrometer in the region of 400–2000 cm^{-1}. A single polyethylene ST-IR card supplied by Fisher Scientific was used for collecting spectra. A glass vial was filled with 6.05 μg/mL SWCNT concentrate in [C_4mpy] [NTf_2] and stirred for at least 10 min. Then, the sample was irradiated with UV light for a total of 180 min using a Stratagene Stratalinker 1800 from Marshall Scientific while oxygen was simultaneously bubbled through the sample. Spectra were recorded at 60 min intervals.

2.6. Electrochemical evaluations for photodynamic effect in SWCNTs/IL system

To prepare the stock suspension for electrochemical measurements, 10 mg of the as-received SWCNTs were added to 10 mL of IL to form a suspension. The suspension was then stirred in the dark for 36 h. The vial was sealed well during the stirring process to prevent the IL from absorbing moisture in the air. The dispersed suspension of SWCNTs and IL was obtained after the stirring and was stored in the dark until further use.

The CV and CA measurements were performed by CH Instruments 660e. For CV measurements, a 2-mm gold electrode was used as the working electrode, and two platinum wires were used as the reference and counter electrode. For CA measurements, a 12.5-μm diameter gold microelectrode was used as the working electrode. The reference and counter electrodes were kept the same. A quartz cuvette cell (transmission range from 170 nm–2700 nm) was used as the electrochemical cell to hold the suspension. The entire setup of the experiments is shown in Fig. 3a.

It consisted of the gas flow system, EC system, and UV lamp. The air-gas from a gas cylinder was dried by an air-drying column (Fisher scientific, Lot No. NC9760623). The flow rate was 100 sccm and controlled by a flow rate controller. A mini magnetic stirrer was added to the cell. A UV lamp (350 nm, 6 Watts) was placed toward the cell at a fixed position.

To prepare the electrolyte, 1.5 mL pure IL and 0.1 mL stock suspension were added to the cell. The concentration of SWCNTs in the IL was about 62.5 μg/ml. The cell was then dried in a vacuum oven at 60 °C overnight to remove moisture in the IL. Air was purged through the system prior to CV measurements; then, the electrochemical cell was stabilized for another 30 min. For all subsequent procedures, the airflow was purged to the surface of the IL rather than into the IL, and the electrolyte was stirred by a magnetic bar to avoid the aggregation of the SWCNTs. The power of the stirring was kept as low as possible to avoid any interference with the electrochemical process. Control group tests were performed by replacing the SWCNTs/IL suspension with pure IL and repeating the same procedures.

3. Results and discussion

In this section, the sustainability of the SWCNTs/IL system under long-term UV light treatment will first be discussed in Section 3.1. The qualitative studies of O_2^- generated from SWCNTs in the IL is provided in Section 3.2. Then, a new method was established to *in-situ* monitor the O_2^- level in the IL system, which is introduced in Section 3.3. Finally, the concentration of O_2^- was quantitively determined through conventional electrochemical methods in Section 3.4.

3.1. Sustainability studies for SWCNTs/IL system by optical spectra characterizations

To investigate the irradiation response of SWCNTs, the UV-VIS absorption spectra of SWCNTs from 300 nm to 1100 nm were obtained (Fig. S1). It has been established that optical absorption spectra can identify SWCNT types [34]. The absorptions at different wavelengths originate from the photo energy requirements for the electronic transitions of M_{11}, E_{11}, and E_{22} (Fig. 1). From the spectra, the SWCNTs showed absorption at the UV range (300−400 nm) and had additional peaks at 587 nm and 1022 nm, which means irradiations at these ranges could be used to excite the SWCNTs. To take full advantage of all mixture types of SWCNTs, a 350 nm UV lamp was used for excitation. Moreover, combining these results with CV and CA data, it was determined that the 350 nm UV irradiation did not change the electrochemical properties of the IL (Section 3.3).

To further confirm the IL had no molecular structural changes after UV illumination, FT-IR absorption spectra for the SWCNTs/IL suspension in the region 400−1500 cm^{-1} was also obtained (Fig. 2a). The intense bands at 740 and 790 cm^{-1} are contributed by S−N stretching and CF_3 bending vibrations, respectively, which aligned well with a previous report [35]. After 3 h of UV treatment, neither new bands appeared nor did any existing bands disappear, which indicated the molecular structure of the IL did not change due to irradiation. Further, this suggested that the IL could be reusable to some extent, showing the excellent sustainability of the system. The noise in the spectra was most likely caused by the presence of SWCNTs, which were black and had strong absorption across the full spectrum.

To investigate the long-term stability of O_2^- in the IL, O_2^- was specifically generated by CV, which has previously been reported as a reliable generation method [30]. The experimental details are given in SI. The existence of CV generated O_2^- was confirmed using UV−vis spectroscopy where an absorbance peak occurred at 235 nm (Fig. S2), which was consistent with other work [29]. The intensity of the absorbance at 235 nm was used to estimate the concentration of O_2^-. As it shown in Fig. 2b, there was 79.7% of O_2^- still remaining in the IL after 65 h, this proved that the IL, [C_4mpy][NTf_2], is an ideal media for storing O_2^- and its high sustainability for the system.

3.2. Qualitative determinations for O_2^- generated by photodynamic effect

To qualitatively confirm the system could generate O_2^- by photodynamic effect, EPR spectroscopy was used to characterize a UV-treated SWCNTs/IL suspension. As it shown in Fig. 2c, the EPR spectrum of the UV-treated SWCNTs/IL suspension showed a single peak at around 3350 G, which was in agreement with other works [36,37]. Thus, the EPR spectra directly confirmed that O_2^- could be generated by SWCNTs via photodynamic effect.

The existence of O_2^- generated solely by SWCNTs was also confirmed by another conventional method using NBT^{2+} as an indicator. NBT^{2+} can react with O_2^- to generate a purple product, monoformazan. The formation of this product is indicated by an optical absorption peak around 530 nm, which can be detected by UV−vis spectroscopy [17]. Since the IL used here was aprotic, a small volume of ethanol was added to the reaction mixture as a proton source that is required to form the final product [38]. The addition of ethanol also improved the solubility of monoformazan compared to that in pure IL; this was especially beneficial since the mixture exhibited the better optical absorption results. As shown in Fig. 2d, the color of both #2 and #5 samples became purple with increasing UV illumination time. Both showed optical absorption at around 530 nm and the intensities of the absorptions increased with UV illumination time. All of these features were consistent with previously reported results [17]. The intensity of #5 was much larger than #2 (Fig. 2e), which confirmed the generation of superoxide by the photodynamic effect of SWCNTs, as only #5 contained SWCNTs. Samples #3 and #6 were placed in a dark room so that the SWCNTs could not utilize photon energy to generate O_2^-, and no color change occurred. These results further confirmed the existence of O_2^- and demonstrated the correlation of O_2^- generated in the system and UV irradiation.

3.3. In-situ monitor for O_2^- level in SWCNTs/IL system

To confirm the SWCNTs/IL system could be evaluated by electrochemical methods, CV measurements were performed in pure IL and in the SWCNTs/IL suspension at various scan rates. Figs. 3b and d show typical CV curves obtained for the pure IL and the suspension of SWCNTs and IL at room temperature, respectively, where the curve has a forward reduction peak (labeled by ①) and a backward oxidation peak (labeled by ②). Ideally, when no other impurities were present, the O_2 was reduced to O_2^- in the reduction process, and the O_2^- was oxidized back to O_2 in the oxidation process. The presence of the oxidation peak (②) suggested the existence of O_2^-. The peak potential for O_2^- generation was −0.73 V (vs. Fc+/Fc). The CV curves in pure IL contained 0.01 M ferrocene and are shown in Fig. S3. The features of the curve in pure IL were identical to that in the suspension, which indicated that the SWCNTs were not involved in the electrochemical process. The curve also aligns well with other works that used the same IL [27,30].

The CVs for the IL contained no SWCNTs or contained SWCNTs were performed at scan rates of 9, 36, 64, 81, and 100 mV/s. The results are provided in Figs. 3b and d. It was found that the separation between the reduction and oxidation peak potentials changed with the scan rate (Table 1), which indicated the

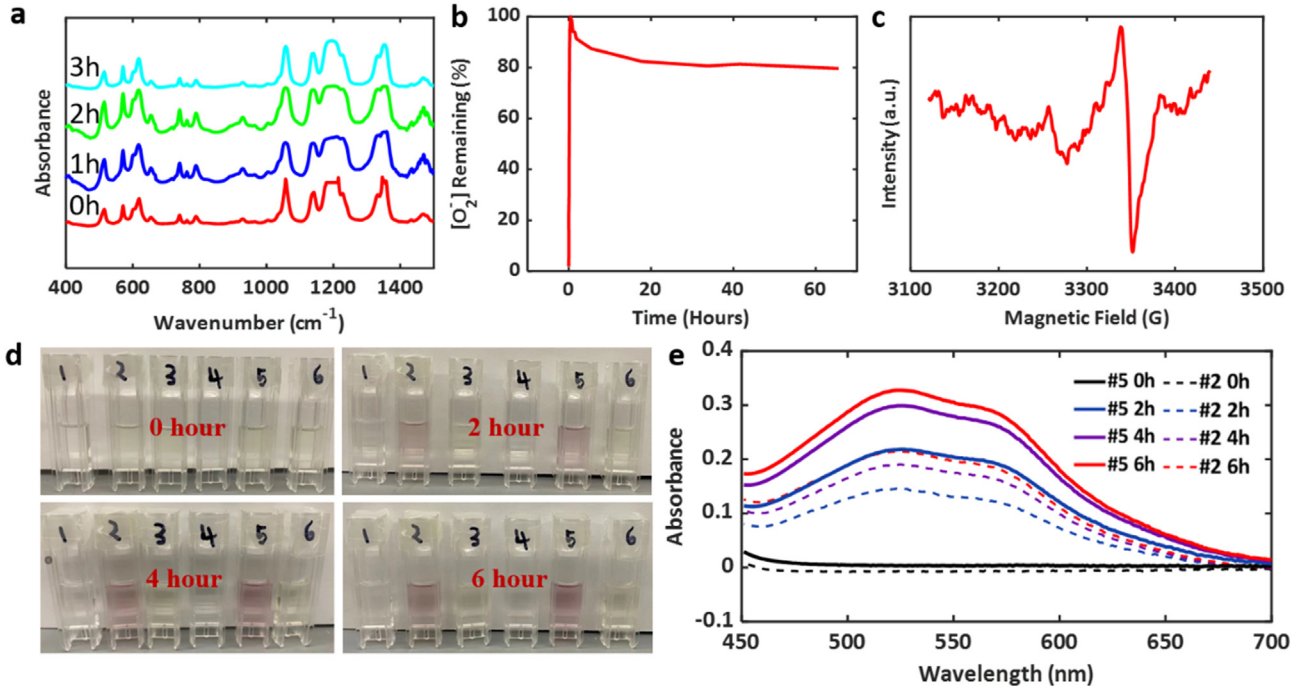

Fig. 2. Sustainability characterization for the SWCNTs/IL system and qualitative studies of O_2^- in the system. (a) FT-IR absorbance spectra for the suspension of IL and SWCNTs with UV light treatment after 0, 1, 2, and 3 h. (b) The percentage of O_2^- remaining in the IL vs. time. (c) EPR spectrum of O_2^- generated by SWCNTs/IL suspension after 24 h of UV light treatment. (d) UV–visible absorption spectra of the SWCNTs/IL system containing NBT^{2+}. (e) Color change after 0, 2, 4, and 6 h for samples of #1. IL and ethanol; #2. IL, NBT^{2+} and ethanol (350 nm UV radiation); #3. IL, NBT^{2+}, and ethanol (dark). #4. IL, SWCNTs, and ethanol; #5. IL, NBT^{2+}, SWCNTs, and ethanol (350 nm UV radiation); #6. IL, NBT^{2+}, SWCNTs, and ethanol (dark). EPR, electron paramagnetic resonance; FT-IR, Fourier-transform infrared; IL, ionic liquid; NBT, nitro blue tetrazolium; SWCNT, single-walled carbon nanotube; UV, untraviolet.

electrochemical generation of O_2^- was an irreversible process. The peak currents for the reduction and oxidation processes are proportional to the square root of the scan rate (Fig. 3c and e), which confirmed the electrochemical process is under diffusion control. This is also consistent with an irreversible electrochemical process [30,33]. These results proved that the SWCNTs/IL system could be evaluated and analyzed by electrochemical methods.

To establish an *in-situ* detection method for O_2^- in the SWCNTs/IL system, long-term, continuous CVs were performed while the system was simultaneously under UV irradiation. Three other samples were setup as control groups, including IL under UV treatment (IL UV), SWCNTs/IL without UV treatment (SWCNTs/IL no UV), and IL without UV treatment (IL no UV). Since the oxygen redox process in IL was under diffusion control, the oxidation peak current, $i_{po,}$ is positively correlated to three parameters, the concentration of O_2^- ($[O_2^-]$), the diffusion coefficient of O_2^-, and the scan rate of CVs [39]. The diffusion coefficient of O_2^- can be considered constant if the temperature is constant, thus, when using the same scan rate to perform the CVs, i_{po} is proportional to $[O_2^-]$. As such, the peak current density is an important factor used to estimate $[O_2^-]$.

The kinetics of the photodynamic effect were explored using the change of peak current densities with reaction time. Fig. 4a shows the peak current density changes o vs. the reaction time in pure IL electrolyte without UV illumination. It was found that both reduction and oxidation current densities exhibited a slight increase, which suggested that O_2 dissolved in the IL and was reduced to O_2^- in the CV process. This was consistent with previous reports [27,30,39]. When the pure IL electrolyte was illuminated by UV light (Fig. 4b), the reduction peak current densities of O_2 dramatically decreased while the oxidation current densities of O_2^- continued to increase. This was because the slight increase of temperature caused by UV illumination increased the diffusion coefficient of O_2 in the IL and facilitated the reduction reaction of O_2 to produce more O_2^-. The decrease of the concentration of O_2 ($[O_2]$) in the IL leads the reduction of current densities to decrease during the first half of scanning. We believe that the ability of O_2 from air to dissolve in IL is weak and slow. Though the air was purging to the surface of IL, the local $[O_2]$ near the working electrode was decreased in the first 5 h. Thus, O_2 was rapidly consumed, and O_2^- was rapidly generated in the first 5 h. Later, the consumption and compensation of O_2 reached dynamic equilibrium. The reduction current densities no longer decreased, and the increased rate of the oxidation current densities was also smaller than the first 5 h. This indicated that the $[O_2]$ was stable, and the increased rate of O_2^- became slower after 5 h.

When SWCNTs were added to the IL in the dark (Fig. 4c), the reduction and oxidation current densities exhibited a similar increase to that in Fig. 4a. This indicated that the presence of SWCNTs in the electrolyte did not change the electrochemical system. This was consistent with previous CV experiments using various scan rates (Fig. 3). When the electrolyte suspension was treated with 350 nm UV light (Fig. 4d), the reduction current densities only decreased for a short period of time (1–3 h) and then slightly increased. This was similar to the case in Fig. 4b and proved the repeatability of the different experiments. The oxidation current densities show a significant increase in Fig. 4d, which suggests the $[O_2^-]$ was greatly increased by the photodynamic effect.

Herein we have established a new method to *in-situ* monitor the relative O_2^- levels in the SWCNTs/IL system. Based on the fundamentals of electrochemistry, peak current is correlated to the concentration of reactant [33]. Here, the ratio of oxidation peak current to reduction peak current ($R = i_{po}/i_{pr}$) was used to evaluate the generation of O_2^- from the photodynamic effect of SWCNTs. i_{po} is correlated to $[O_2^-]$ in the IL overall, and i_{pr} is correlated to the $[O_2]$

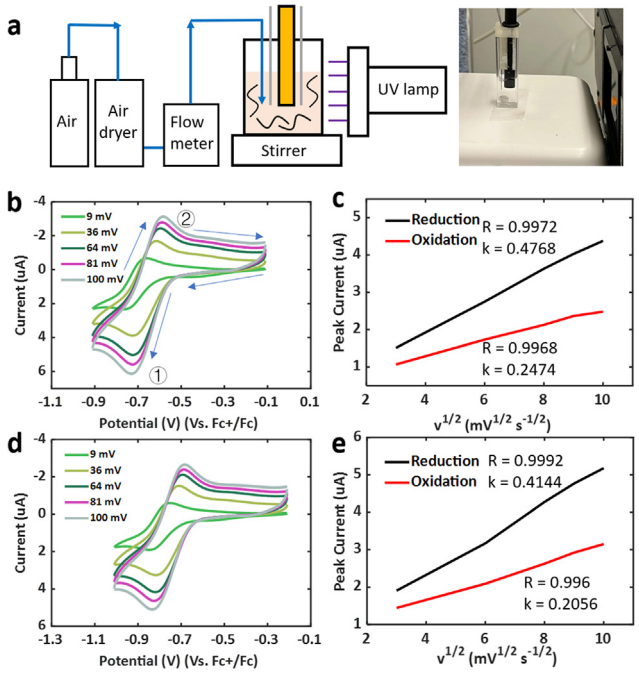

Fig. 3. Electrochemical reaction cell setup and CV curves at various scan rates. (a) reaction cell setup. (b) and (c) CVs for IL in the absence of SWCNTs at room temperature and scan rates of 9, 36, 64, 81, and 100 mV/s (d) and (e) CVs for IL in the presence of SWCNTs and IL suspension at room temperature and scan rates of 9, 36, 64, 81, and 100 mV/s. CV, cyclic voltammetry; IL, ionic liquid; SWCNT, single-walled carbon nanotube.

that was involved in the reduction reaction where a small amount of O_2^- was chemically generated. Thus, the defined R could be used to evaluate the $[O_2^-]$ distinctly generated by SWCNTs in the system and excluding any O_2^- produced from electrochemical reaction.

Considering the increase of O_2^- led to the oxidation reaction during CV to produce O_2, such a contribution of O_2 would likewise increase i_{pr} during the reduction process. Thus, a constant i_{pr}, when $t = 0$, was used for calculations and is represented by $i_{pr}(0)$; i_{po} is given as a function of reaction time and is represented by $i_{po}(t)$. As a result, R(t) is given by Eq. (1).

$$R(t) = i_{po}(t)/i_{pr}(0) \quad (1)$$

To make comparisons among control groups and experimental groups, R(t) was normalized by Eq. (2):

$$C(t) = \frac{R(t) - R(0)}{R(0)} \quad (2)$$

Where C(t) represented the relative $[O_2^-]$ generated by SWCNTs as a function of reaction time. The *in-situ* monitoring results are provided in Fig. 4e. The overall growth trend for the red curve (SWCNTs/IL with UV light) was much larger than the other three curves. This confirmed the generation of O_2^- by SWCNTs when illuminated with UV light since the normalized ratio did not increase when UV illumination ('SWCNTs/IL no UV') or SWCNTs ('IL UV') were absent. Besides, it has been reported that metal catalyst from CNTs was involved in the formation of ROS, such as Nickle [17]. However, the 'SWCNTs/IL no UV' curve was on similar level as the other two control groups. It indicated that the SWCNTs/IL system could not generate O_2^- in absence of UV light. This was consistent with the result from NBT^{2+} characterization and ruled out the possibility that the catalyst metal from SWCNTs was involved in the reaction. In fact, the sample used in this work was highly purified SWCNTs. After 100-fold dilution, the concentrations of other impurities were even lower. Thus, the catalyst metal has negligible impact on the system. Comparing the 'IL UV' curve with the 'IL no UV' curve, it was found that UV illumination slightly facilitated the reduction reaction of O_2. The slight increase of temperature caused by the UV illumination increased the diffusion coefficient of O_2, which was consistent with the current density analysis discussed previously. When both SWCNTs and UV illumination existed ('SWCNTs UV' curve), O_2^- was quickly generated, and the $[O_2^-]$ under these conditions was much larger than that of control groups. This demonstrated the photodynamic effect of SWCNTs when the system was illuminated with UV light. The newly established method was able to in-situ monitor the O_2^- level in the SWCNTs/IL or pure IL system.

3.4. Quantitative determination of O_2^- by conventional electrochemical measurements

$[O_2^-]$ was quantitatively determined by both CV and CA measurements using a 2-mm and 12.5 μm gold microelectrode, respectively, via conventional electrochemical calculations. According to Hayyan et al. and Katayama et al. [39,40], for an irreversible, one-step, and one-electron electrochemical reaction ($O_2 + e \rightarrow O_2^-$), the peak current and potential from CV measurements are given by the following Eqs. (3)–(5) [33]:

$$i_{pr} = \left(2.99 * 10^5\right) \alpha^{1/2} A C_o D_o{}^{1/2} \nu^{1/2} \quad (3)$$

$$\left|E_p - E_{p/2}\right| = \frac{1.857RT}{\alpha F} \quad (4)$$

Where α is charge transfer coefficient; A is the surface area of the working electrode in cm^2; C_o is the bulk concentration of O_2 in mol/ml; D_o is diffusion coefficient of O_2 in cm^2/s; ν is scan rate in V/s; E_p is the peak potential in V; $E_{p/2}$ is the half-peak potential in V; R is the universal gas constant in J/(mol. K); T is the absolute temperature in K; F is Faraday's constant, 96,485 C/mol.

Table 1
Peak-to-peak potential separation at various scan rates.

Scan rate (mV/s)	$\lvert E_{pr} - E_{po}\rvert$ (mV)		$\lvert E_p - E_{p/2}\rvert$ (mV)	$\lvert E_p - E_{p/2}\rvert$ (mV)
	IL	IL + SWCNTs	IL	IL + SWCNTs
9	103	96	79	88
36	111	106	103	100
64	134	128	103	100
81	139	138	101	104
100	151	151	101	103

$\lvert E_{pr} - E_{po}\rvert$: The difference between reduction peak and oxidation peak potential.
$\lvert E_p - E_{p/2}\rvert$: The difference between reduction peak and half reduction peak potential.

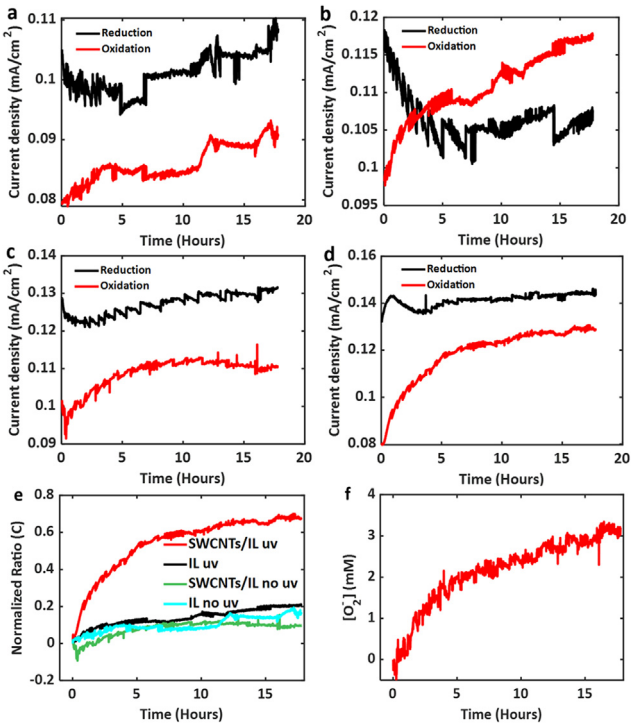

Fig. 4. The reduction and oxidation peak current density changes in (a) pure IL (dark), (b) pure IL (UV), (c) SWCNTs/IL (dark), (d) SWCNTs/IL (UV). (e) *In-situ* monitor of O_2^- levels in SWCNTs/IL and IL systems. (f) [O_2^-] generated by SWCNTs vs. reaction time. IL, ionic liquid; SWCNT, single-walled carbon nanotube.

From CA measurements, the steady-state current (i_{ss}) was obtained (Fig. S4) and given as follows:

$$i_{ss} = 4nFD_oC_or_o \quad (5)$$

Where n is the number of electrons and r_o is the radius of the electrode. Consequently, C_o and D_o can be solved using Eqs. (3)–(5). As shown in Table 2, [O_2] was smaller in the suspension than in pure IL, but the diffusion coefficient of O_2 for the suspension and IL were inversely related. This suggested SWCNTs absorbed a portion of O_2 molecules that dissolved in the IL. During the forward voltage scan, the dissolved O_2 molecules diffused to and were reduced at the working electrode, considering this, SWCNTs might also be driven to the electrode. The evidence suggested SWCNT aggregation occurred during long-term CV measurements. The conductive and tiny SWCNTs may diffuse faster than O_2 when driven by voltage. As a result, the diffusion coefficient of O_2 increases.

If Eq. (3) is applied to both reduction and oxidation processes and substituted into R, Eq. (6) is given by:

$$R = i_{po}/i_{pr} = C_xD_x/C_o\ D_o \quad (6)$$

Where C_x is [O_2^-], and D_x is the diffusion coefficient of O_2^-. The diffusion coefficient of O_2^- in this IL is constant and was taken from the literature [39]. In Eq. (6), C_o and D_o can be obtained by Eqs. (1) and (3), which is given in Table 2. C_o was assumed to be constant since the air was continuously purged into the electrochemical cell. D_r and D_o were also assumed to be constant, as they were only dependent on temperature. Thus, using Eq. (6), the [O_2^-] for all four samples, SWCNTs/IL UV, IL UV, SWCNTs/IL no UV, and IL no UV, was determined. After calculations, the initial [O_2^-] was normalized to zero mM at time zero. The [O_2^-] generated by SWCNTs changed with reaction time and is given in Fig. 4**f**, where the electrochemically generated [O_2^-] has already been subtracted.

Table 2
Concentration of O_2 (C_o), diffusion coefficient of O_2 (D_o), steady-state current (i_{ss}), charge transfer coefficient (α) in suspension, and pure IL.

	C_o (mmol)	D_o (10^{-9} m^2/s)	α	i_{ss} (nA)
Suspension	0.43	2.8	0.36	2.897
IL	1.33	0.33	0.44	1.070

Based on Fig. 4f, the SWCNTs/IL system generated 4.11 mM of O_2^- within 17 h. We were aware that the CV process could generate a small amount of O_2^-. After subtracting the partial concentration of O_2^- from CV, the total amount of O_2^- from photodynamic effect was determined to be 3.19 mM. In the first 60 min, the SWCNTs/IL system produced 190 μM of O_2^-, which was more than six times greater than a recently reported ROS generator that produced 29.62 μM of O_2^- in 60 min [3]. Meanwhile, the reaction rate constant ($k_0 = d[O_2^-]/dt$) for the photodynamic effect was determined to be $4.99 * 10^{-8}$ mol·L^{-1}·s^{-1}. This exhibited a high generation efficiency of O_2^- in this system. Taking the weight of SWCNTs (62.5 μg/ml) into consideration, k_0 was determined to be $4.99 * 10^{-4}$ mol·L^{-1}·g^{-1}·s^{-1}. The generated O_2^- herein was still excessive with respect to the germicidal levels of ROS [3,41]. Given the small scale of this system, which only contained 1.6 mL IL and 0.1 mg SWCNTs, it is expected the generation efficiency could be improved by enlarging the scale of the system—adding more SWCNTs and adjusting the wavelength of illumination. The low-level detection of [O_2^-] by electrochemical techniques could provide feedback for those improvements and help optimize the system in future research.

4. Conclusions

This study illustrates the newly developed SWCNTs/IL ([C_4mpy][NTf_2]) suspension is a sustainable system to efficiently produce and store ROS for long-term. The photodynamic effect of SWCNTs could enable high-yield O_2^- generation in non-aqueous, IL media under UV illumination. The generation of O_2^- by SWCNTs in the IL was qualitatively confirmed by UV–vis and EPR spectroscopy, as well as electrochemical measurements. The IL was confirmed to have no structural changes after long-term UV light treatment. Based on CV measurements, the SWCNTs/IL system works with electrochemical methods, which enable *in-situ* monitoring of O_2^-. To the best of our knowledge, this is the first time generating O_2^- by SWCNTs in IL without interference from water, and *in-situ* monitored O_2^- levels by CV has been reported. This new suspension system could be used as an effective generator and sustainable storage media for O_2^-, as well as a real-time *in-situ* monitor for the low-level detection of O_2^-. The system could also be used as a starting point for generating O_2^- using other materials in the future. It is expected that this work will help elucidate the kinetics of ROS generation using carbon materials and pave the way for their applications in air and water disinfection and O_2^- sensitive chemical sensors.

Declaration of competing interest

The authors declare they have no known competing financial interests or personal relationships that could have appeared to influence the work reported in this paper.

Acknowledgments

P. D. acknowledges the financial support from the Department of the Interior, Bureau of Reclamation under contract R19AC00116, and the Idaho National Laboratory Directed Research &

Development program under the Department of Energy Idaho Operations Office Contract DE-AC07-051D14517. Z.W. acknowledges the financial support from Army Research Office (W911NF-18-1-0458), and National Science Foundation (CHE-1832167).

Appendix A. Supplementary data

Supplementary data to this article can be found online at https://doi.org/10.1016/j.mtsust.2022.100171.

References

[1] Y. Zhao, Z.-X. Low, Y. Pan, Z. Zhong, G. Gao, Universal water disinfection by piezoelectret aluminium oxide-based electroporation and generation of reactive oxygen species, Nano Energy 92 (2022) 106749, https://doi.org/10.1016/j.nanoen.2021.106749.
[2] A. Samanta, S. Ghosh, S. Sarkar, Sustained generation of peroxide from the air by carbon nano onion under visible light to combat RNA virus, J. Chem. Sci. 134 (2022) 9, https://doi.org/10.1007/s12039-021-02013-1.
[3] T. Cao, W. Tong, F. Feng, S. Zhang, Y. Li, S. Liang, X. Wang, Z. Chen, Y. Zhang, H_2O_2 generation enhancement by ultrasonic nebulisation with a zinc layer for spray disinfection, Chem. Eng. J. 431 (2022) 134005, https://doi.org/10.1016/j.cej.2021.134005.
[4] P. Sharma, A.B. Jha, R.S. Dubey, M. Pessarakli, Reactive oxygen species, oxidative damage, and antioxidative defense mechanism in plants under stressful conditions, J. Bot., Le 2012 (2012) 1–26, https://doi.org/10.1155/2012/217037.
[5] M. Hayyan, M.A. Hashim, I.M. Alnashef, Superoxide ion: generation and chemical implications, Chem. Rev. 116 (2016) 3029–3085, https://doi.org/10.1021/acs.chemrev.5b00407.
[6] J. Zhang, M. Zhang, L. Qiu, Y. Zeng, J. Chen, C. Zhu, Y. Yu, Z. Zhu, Three-dimensional interconnected core-shell networks with Ni(Fe)OOH and M-N-C active species together as high-efficiency oxygen catalysts for rechargeable Zn-air batteries, J. Mater. Chem. A. 7 (2019) 19045–19059, https://doi.org/10.1039/c9ta06852j.
[7] S. Zhao, L. Ban, J. Zhang, W. Yi, W. Sun, Z. Zhu, Cobalt and nitrogen co-doping of porous carbon nanosphere as highly effective catalysts for oxygen reduction reaction and Zn-air battery, Chem. Eng. J. 409 (2021) 128171, https://doi.org/10.1016/j.cej.2020.128171.
[8] F.L. Michael, De Volder, H. Sameh, Ray H. Tawfick, A. Baughman, John ;hart, carbon nanotubes: present and future commercial applications, Science 339 (2013) 535–539.
[9] R. He, X. Huang, M. Chee, F. Hao, P. Dong, Carbon-based perovskite solar cells: from single-junction to modules, Carbon Energy 1 (2019) 109–123, https://doi.org/10.1002/cey2.11.
[10] Y. Che, H. Chen, H. Gui, J. Liu, B. Liu, C. Zhou, Review of carbon nanotube nanoelectronics and macroelectronics, Semicond. Sci. Technol. 29 (2014), https://doi.org/10.1088/0268-1242/29/7/073001.
[11] V.K.K. Upadhyayula, S. Deng, M.C. Mitchell, G.B. Smith, Application of carbon nanotube technology for removal of contaminants in drinking water: a review, Sci. Total Environ. 408 (2009) 1–13, https://doi.org/10.1016/j.scitotenv.2009.09.027.
[12] S. Park, M. Vosguerichian, Z. Bao, A review of fabrication and applications of carbon nanotube film-based flexible electronics, Nanoscale 5 (2013) 1727–1752, https://doi.org/10.1039/c3nr33560g.
[13] J. Zhao, D. Wei, C. Zhang, Q. Shao, V. Murugadoss, Z. Guo, Q. Jiang, X. Yang, An overview of oxygen reduction electrocatalysts for rechargeable zinc-air batteries enabled by carbon and carbon composites, Eng. Sci. 15 (2021) 1–19, https://doi.org/10.30919/es8d420.
[14] X. Huang, R. He, M. Li, M.O.L. Chee, P. Dong, J. Lu, Functionalized separator for next-generation batteries, Mater. Today 41 (2020) 143–155, https://doi.org/10.1016/j.mattod.2020.07.015.
[15] J. Zhang, M. Zhang, Y. Zeng, J. Chen, L. Qiu, H. Zhou, C. Sun, Y. Yu, C. Zhu, Z. Zhu, Single Fe atom on hierarchically porous S, N-codoped nanocarbon derived from porphyra enable boosted oxygen catalysis for rechargeable Zn-air batteries, Small 15 (2019) 1–11, https://doi.org/10.1002/smll.201900307.
[16] A. Joshi, S. Punyani, S.S. Bale, H. Yang, T. Borca-Tasciuc, R.S. Kane, Nanotube-assisted protein deactivation, Nat. Nanotechnol. 3 (2008) 41–45, https://doi.org/10.1038/nnano.2007.386.
[17] C.Y. Chen, C.T. Jafvert, Photoreactivity of carboxylated single-walled carbon nanotubes in sunlight: reactive oxygen species production in water, Environ. Sci. Technol. 44 (2010) 6674–6679, https://doi.org/10.1021/es101073p.
[18] X. Qu, P.J.J. Alvarez, Q. Li, Photochemical transformation of carboxylated multiwalled carbon nanotubes: role of reactive oxygen species, Environ. Sci. Technol. 47 (2013) 14080–14088, https://doi.org/10.1021/es4033056.
[19] H.S. Hsieh, R. Wu, C.T. Jafvert, Light-independent reactive oxygen species (ROS) formation through electron transfer from carboxylated single-walled carbon nanotubes in water, Environ. Sci. Technol. 48 (2014) 11330–11336, https://doi.org/10.1021/es503163w.
[20] M.M. Safaee, M. Gravely, D. Roxbury, A wearable optical microfibrous biomaterial with encapsulated nanosensors enables wireless monitoring of oxidative stress, Adv. Funct. Mater. 31 (2021) 1–14, https://doi.org/10.1002/adfm.202006254.
[21] T. Vainikka, M.C. Figueiredo, K. Kontturi, L. Murtomäki, Studies of oxygen reduction in 1-butyl-1-methylpyrrolidinium bis(trifluoromethylsulfonyl) imide by microdisk voltammetry, Electrochim, Acta 156 (2015) 60–69, https://doi.org/10.1016/j.electacta.2014.12.172.
[22] C. Backes, Noncovalent Functionalization of Carbon Nanotubes: Fundamental Aspects of Dispersion and Separation in Water, Springer, 2012.
[23] R. Fukuda, T. Umeyama, M. Tsujimoto, F. Ishidate, T. Tanaka, H. Kataura, H. Imahori, T. Murakami, Sustained photodynamic effect of single chirality-enriched single-walled carbon nanotubes, Carbon N. Y. 161 (2020) 718–725, https://doi.org/10.1016/j.carbon.2020.02.002.
[24] Y. Zhang, M. Dai, Z. Yuan, Methods for the detection of reactive oxygen species, Anal. Methods 10 (2018) 4625–4638, https://doi.org/10.1039/c8ay01339j.
[25] J.C. Barreto, G.S. Smith, N.H.P. Strobel, P.A. McQuillin, T.A. Miller, Terephthalic acid: a dosimeter for the detection of hydroxyl radicals in vitro, Life Sci. 56 (1994) 89–96, https://doi.org/10.1016/0024-3205(94)00925-2.
[26] W.R. Haag, J. Hoigné, Photo-sensitized oxidation in natural water via .OH radicals, Chemosphere 14 (1985) 1659–1671, https://doi.org/10.1016/0045-6535(85)90107-9.
[27] Z. Wang, X. Zeng, Bis(trifluoromethylsulfonyl)imide (NTf 2)-based ionic liquids for facile methane electro-oxidation on Pt, J. Electrochem. Soc. 160 (2013) H604–H611, https://doi.org/10.1149/2.039309jes.
[28] Z. Wang, M. Guo, G.A. Baker, J.R. Stetter, L. Lin, A.J. Mason, X. Zeng, Methane–oxygen electrochemical coupling in an ionic liquid: a robust sensor for simultaneous quantification, Analyst 139 (2014) 5140–5147, https://doi.org/10.1039/c4an00839a.
[29] E.I. Rogers, X.J. Huang, E.J.F. Dickinson, C. Hardacre, R.G. Compton, Investigating the mechanism and electrode kinetics of the oxygenlsuperoxide (O_2|O_2^-) couple in various room-temperature ionic liquids at gold and platinum electrodes in the temperature range 298-318 K, J. Phys. Chem. C 113 (2009) 17811–17823, https://doi.org/10.1021/jp9064054.
[30] M. Hayyan, F.S. Mjalli, I.M. AlNashef, M.A. Hashim, Chemical and electrochemical generation of superoxide ion in 1-butyl-1-methylpyrrolidinium bis(trifluoromethylsulfonyl)imide, Int. J. Electrochem. Sci. 7 (2012) 8116–8127.
[31] Z. Wang, S. He, V. Nguyen, K.E. Riley, Ionic liquids as “green solvent and/or electrolyte” for energy interface, Eng. Sci. 11 (2020) 3–18, https://doi.org/10.30919/es8d0013.
[32] S. Angaiah, V. Murugadoss, S. Arunachalam, P. Panneerselvam, S. Krishnan, Influence of various ionic liquids embedded electrospun polymer membrane electrolytes on the photovoltaic performance of DSSC, Eng. Sci. 4 (2018) 44–51, https://doi.org/10.30919/es8d756.
[33] A.J. Bard, L.R. Faulkner, E. Swain, C. Robey, Electrochemical Methods: Fundamentals and Applications, Wiley, (n.d).
[34] X. Tu, S. Manohar, A. Jagota, M. Zheng, DNA sequence motifs for structure-specific recognition and separation of carbon nanotubes, Nature 460 (2009) 250–253, https://doi.org/10.1038/nature08116.
[35] S. Saha, T. Taguchi, N. Tachikawa, K. Yoshii, Y. Katayama, Electrochemical behavior of cadmium in 1-Butyl-1-methylpyrrolidinium bis(trifluoromethylsulfonyl)amide room-temperature ionic liquid, Electrochim. Acta 183 (2015) 42–48, https://doi.org/10.1016/j.electacta.2015.05.018.
[36] J.R. Reddan, F.J. Giblin, M. Sevilla, V. Padgaonkar, D.C. Dziedzic, V.R. Leverenz, I.C. Misra, J.S. Chang, J.T. Pena, Propyl gallate is a superoxide dismutase mimic and protects cultured lens epithelial cells from H2O2 insult, Exp. Eye Res. 76 (2003) 49–59, https://doi.org/10.1016/S0014-4835(02)00256-7.
[37] K. Sobańska, A. Krasowska, T. Mazur, K. Podolska-Serafin, P. Pietrzyk, Z. Sojka, Diagnostic features of EPR spectra of superoxide intermediates on catalytic surfaces and molecular interpretation of their G and A tensors, Top. Catal. 58 (2015) 796–810, https://doi.org/10.1007/s11244-015-0420-y.
[38] G. Bartosz, Use of spectroscopic probes for detection of reactive oxygen species, Clin. Chim. Acta 368 (2006) 53–76, https://doi.org/10.1016/j.cca.2005.12.039.
[39] Y. Katayama, K. Sekiguchi, M. Yamagata, T. Miura, Electrochemical behavior of oxygen/superoxide ion couple in 1-butyl-1-methylpyrrolidinium bis(trifluoromethanesulfone)imide room-temperature molten salt, Proc. - Electrochem. Soc. PV 24 (2006) (2004) 503–512, https://doi.org/10.1149/200424.0503pv.
[40] M. Hayyan, F.S. Mjalli, M.A. Hashim, I.M. Alnashef, S.M. Al-Zahrani, K.L. Chooi, Generation of superoxide ion in 1-butyl-1-methylpyrrolidinium trifluoroacetate and its application in the destruction of chloroethanes, J. Mol. Liq. 167 (2012) 28–33, https://doi.org/10.1016/j.molliq.2011.12.005.
[41] K. Lee, S. Shin, W.J. Lee, D. Choi, Y. Ahn, M. Park, D. Seo, K. Seo, Sunlight-activatable ROS generator for cell death using TiO2/c-Si microwires, Nano Lett. 21 (2021) 6998–7004, https://doi.org/10.1021/acs.nanolett.1c02337.